

Optimization: An Introduction

Tapabrata Ray

MDO Group, UNSW, Canberra.

<http://seit.unsw.adfa.edu.au/research/sites/mdo/index.htm>

Acknowledgements: All former and current postgraduate students, collaborators and funding agencies.

Overview of Optimization

Constrained Optimization

Many Objective Optimization

Shape Optimization Examples

Application Snapshots

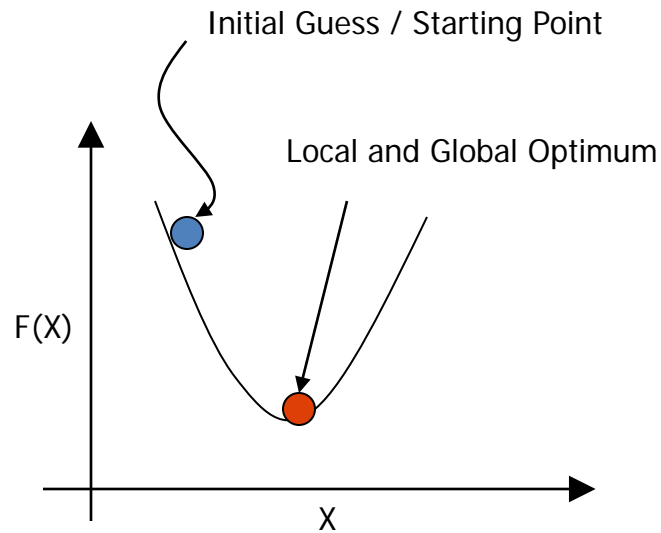


The unusual looking NASA ST5 antenna design was lighter, stronger and consumed less power. (Source: <http://www.nasa.gov/centers/ames/research/exploringtheuniverse/borg.html>).

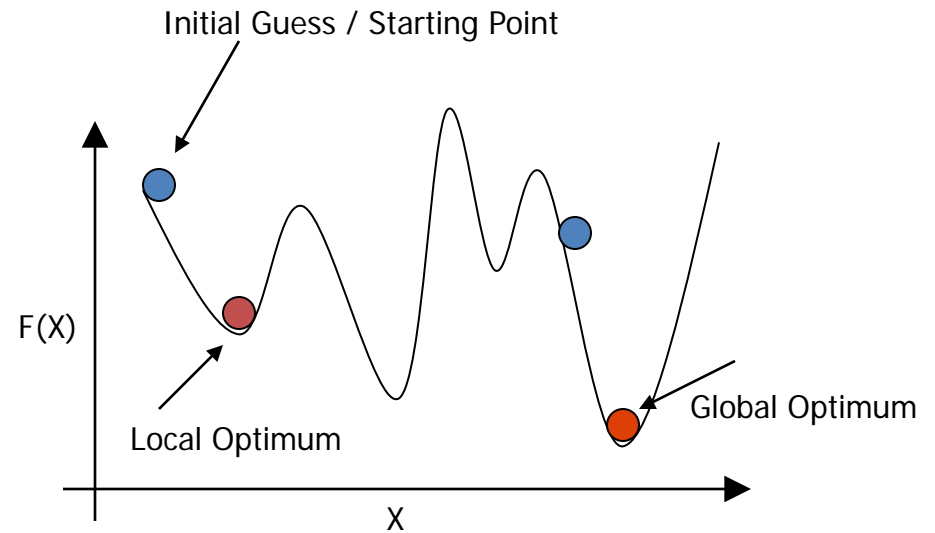
The latest Boeing 787 Dreamliner is claimed to be quieter, more efficient and more environment friendly when compared with existing designs. (Source: <http://www.compositestoday.com/2012/11/boeing-steps-up-787-dreamliner-production/>)

The Mercedes Benz Car design was inspired by drag characteristics of box-fish. (Source: <http://webecoist.momtastic.com/2011/03/21/marine-muse-12-more-sea-inspired-designs-inventions/>)

- Refers to Minimization or Maximization of one or more objectives.
- Variables: Continuous, Discrete, Integers.
- Constraints: Linear, Nonlinear: Inequalities and Equalities.
- Usually in the context of engineering, problems tend to have highly nonlinear objectives and constraints. Such objectives and constraints are often evaluated using computationally expensive simulations.



Unimodal Function



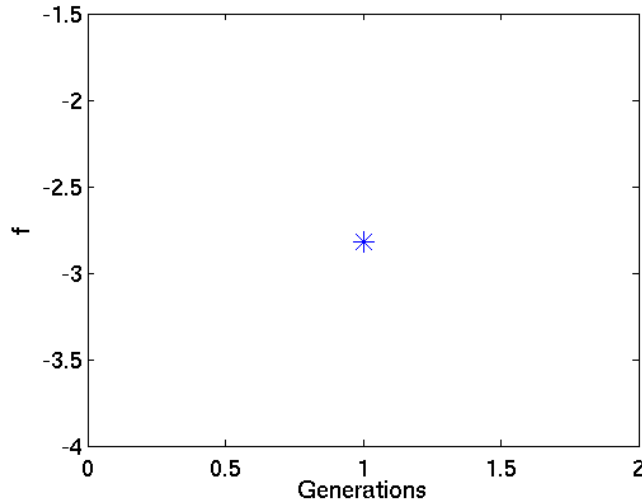
Multimodal Function

No Algorithm Can Guarantee to Locate Global Optimum for Multimodal Functions.

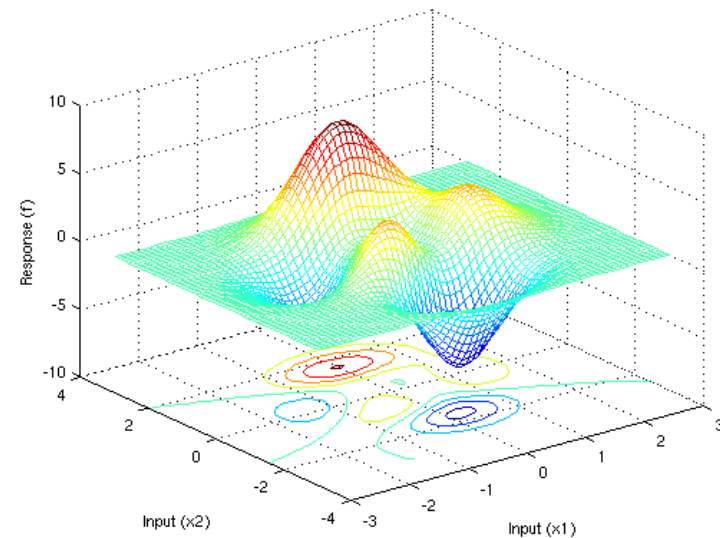
Gradient Based Algorithms Can Guarantee to Locate Local Optimum.

Zero Order Methods Can only Locate a *Good Solution* which may not even be a Local Optimum.

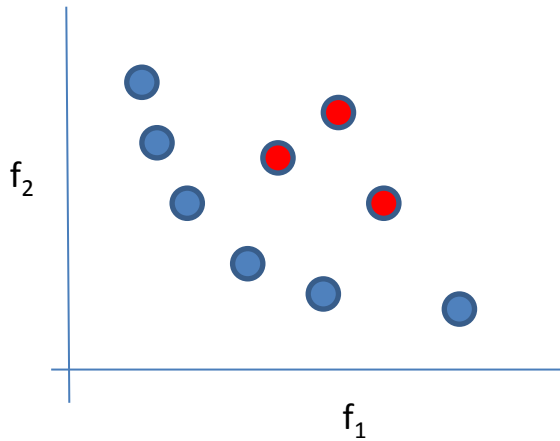
1. Generate a set of M solutions.
2. Identify better solutions as parents.
3. Combine the parents to create M child solutions.
4. Combine the original set of solutions (M) and child solutions (M).
5. Select M solutions from the above set of $2M$ solutions.
6. Repeat steps 2-4 till convergence condition is true.



Progress Plot



Visualization



Minimization and Maximization problems are interchangeable.

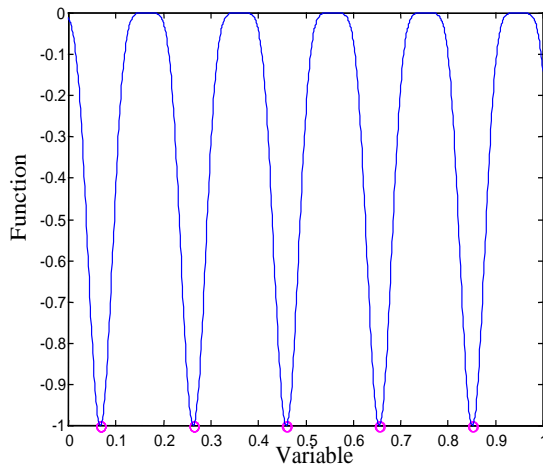
All discussions are in the context of minimization.

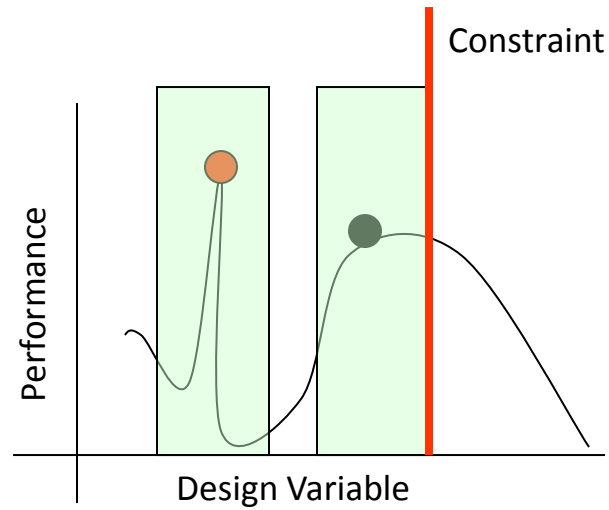
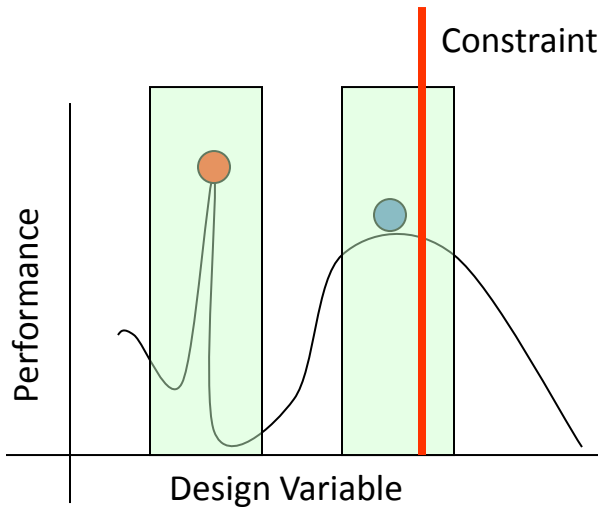
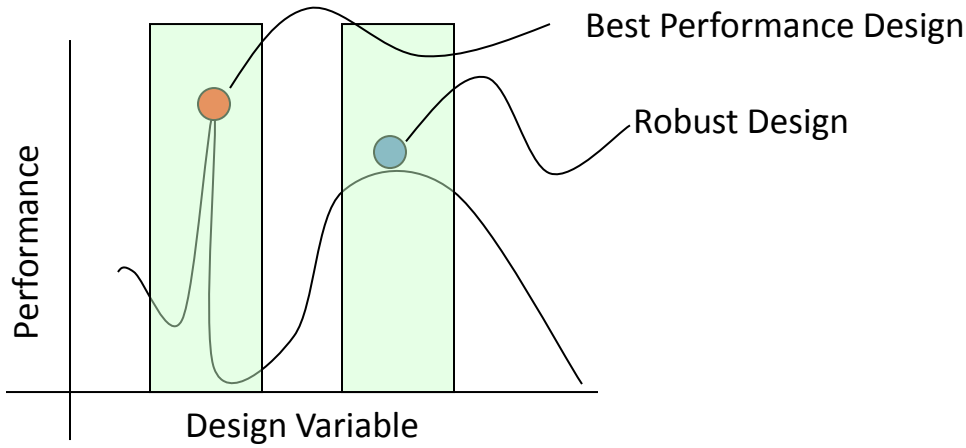
In Multi-objective optimization, the interest is to find the non-dominated set of solutions that are close to the Pareto optimal set.

The ND set of solutions should have a good convergence and a good spread.

The solutions in blue are Non-dominated solutions. The solutions in red are dominated solutions.

Designers are interested in identifying multiple optima.

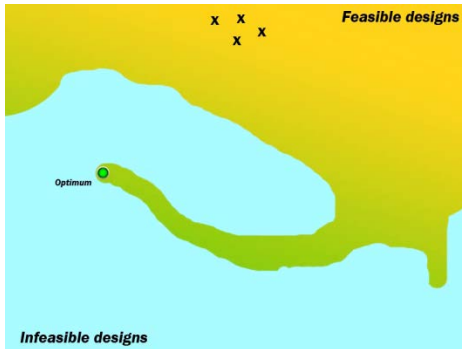




Notice that the Design Shifted away from the Constraint Boundary

Constrained Optimization

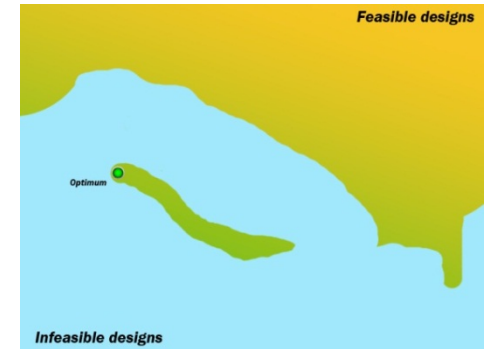
- Solutions to constrained optimization problems often lie on constraint boundaries.
- Most real coded population based stochastic algorithms intrinsically prefer a feasible solution over another.
- Proposed Infeasibility Driven Evolutionary Algorithm (IDEA).



Real coded EA



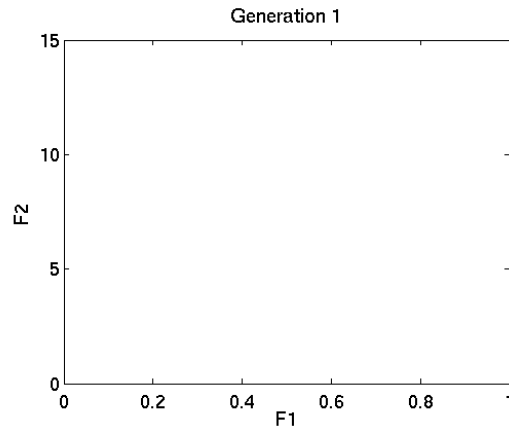
Preserving Infeasible Solutions



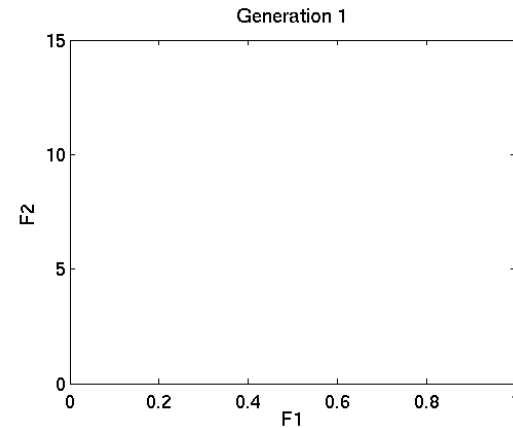
Disconnected Feasible Regions

- Explicitly preserves a fraction of infeasible solutions across generations.
- Marginally infeasible solutions are preferred over feasible solutions.
- Offers a trade-off set of solutions with minimal constraint violation in addition to the set of feasible solutions.

- Behaviour of IDEA on multi-objective optimization problems.



Real coded EA



IDEA

Ray, T., Singh, H.K., Isaacs, A., and Smith, W. Infeasibility Driven Evolutionary Algorithm for Constrained Optimization, *Constraint-Handling in Evolutionary Optimization, Studies in Computational Intelligence Series 198*, Eds, Efrén Mezura-Montes, Springer. pp 145-165., 2009.

Singh, H.K. , Ray, T. and Sarker, R. ,“Optimum oil production planning using infeasibility driven evolutionary algorithm,” *Evolutionary Computation*, In Press, (Accepted 09/201 1).

Many-Objective Optimization

- In order to observe the process of evolution, we computed the average performance of the population i.e. average of the d_1 and d_2 values for the individuals for DTLZ1 (3 objectives)
- One can observe from Fig. 8, that the average d_2 converges to near zero (i.e. near perfect alignment to the reference directions) while the average d_1 measure stabilizes at around 0.8 in the normalized plane indicating convergence to the Pareto front

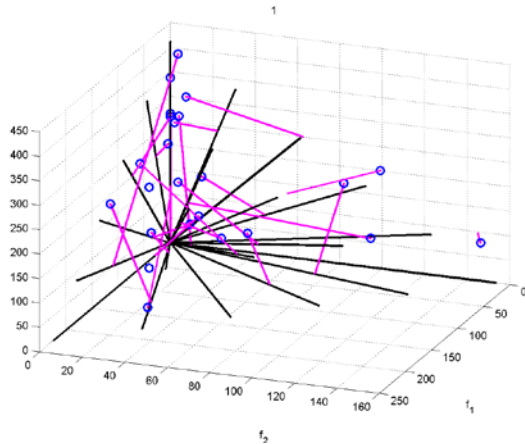


Fig:7. Evolving the best solutions with minimum d_1 and d_2 distances

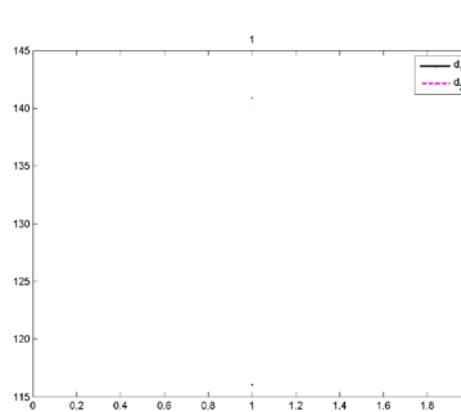


Fig:8. Converging the d_1 and d_2 measures over generations

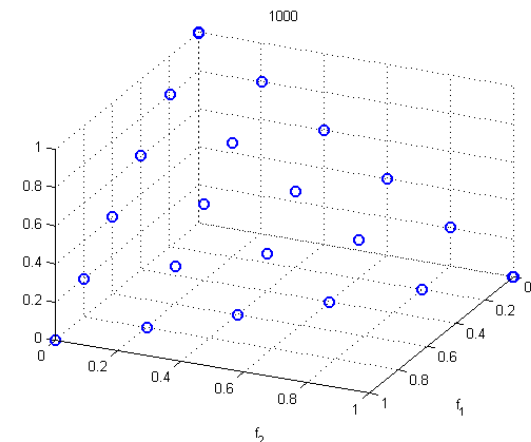
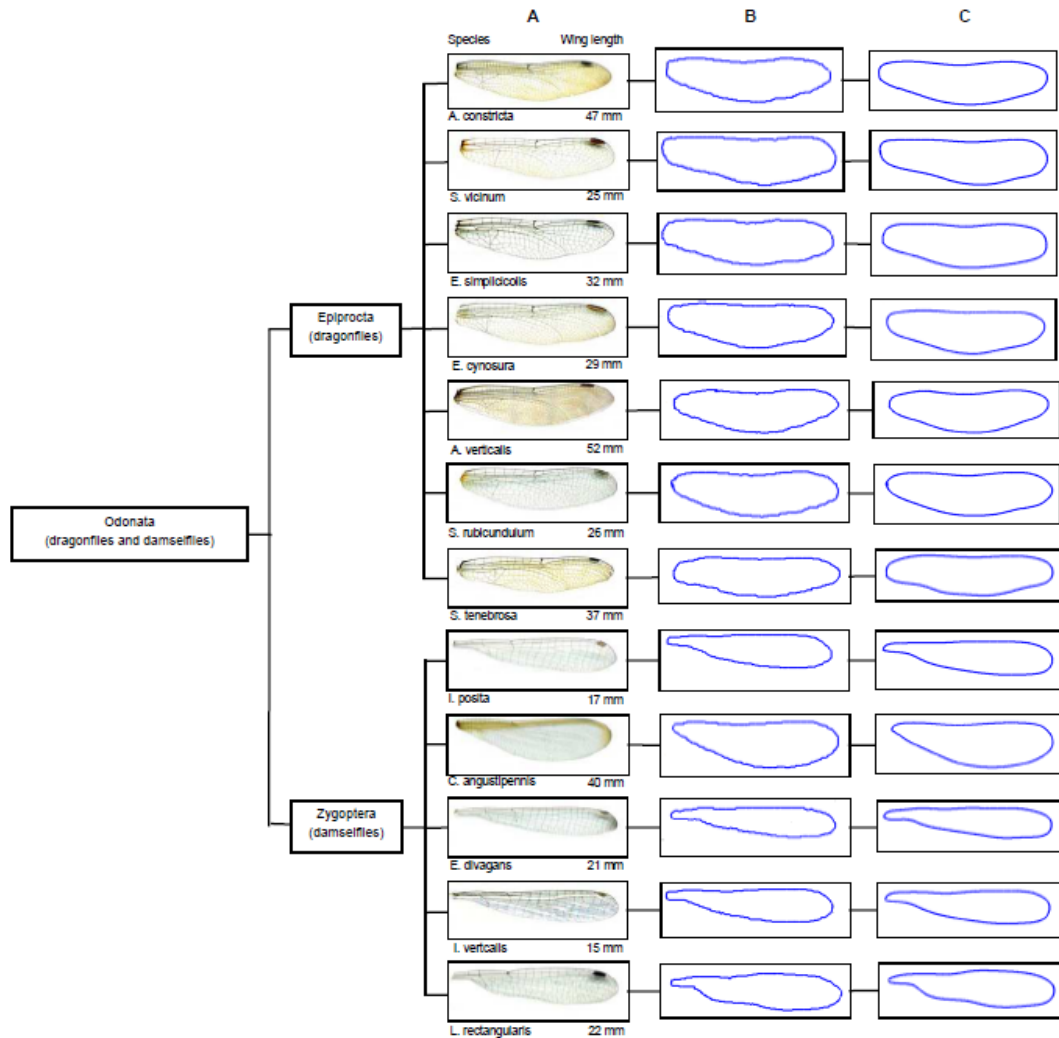


Fig:9. Final non-dominated solutions achieved for DTLZ1 problem

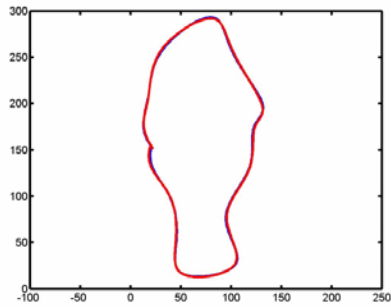
Shape Optimization



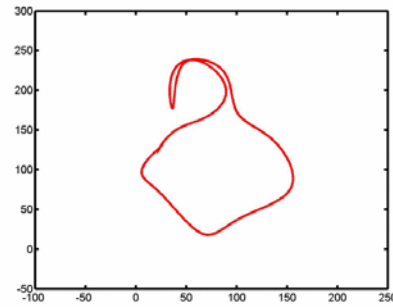
| Species | Length <i>a</i> , mm | Width <i>b</i> , mm | A.ratio <i>a/b</i> |
|-------------------|-------------------------|------------------------|-----------------------|
| A. constricta | 47 | 11.92 | 3.94:1 |
| S. vicinum | 25 | 6.64 | 3.77:1 |
| E. simplicicollis | 32 | 8.21 | 3.89:1 |
| E. cynosura | 29 | 7.64 | 3.79:1 |
| A. verticalis | 52 | 13.69 | 3.79:1 |
| S. rubicundulum | 26 | 6.69 | 3.88:1 |
| S. tenebrosa | 37 | 8.54 | 4.33:1 |
| I. posita | 17 | 3.36 | 5.06:1 |
| C. angustipennis | 40 | 10.76 | 3.71:1 |
| E. divagans | 21 | 3.59 | 5.84:1 |
| I. verticalis | 15 | 2.88 | 5.20:1 |
| L. rectangularis | 22 | 4.68 | 4.70:1 |

Fig.6 Dragonfly and Damselfly wing dimensions with their aspect ratios

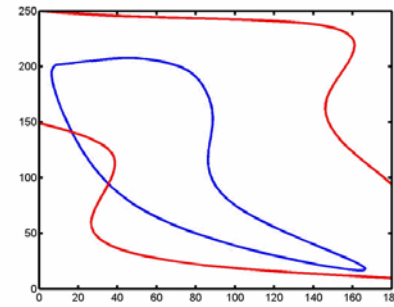
Fig.5 Dragonfly and Damselfly wing species and digitally extracted shapes' boundaries.



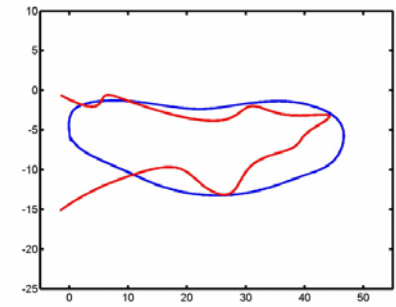
Simple fish



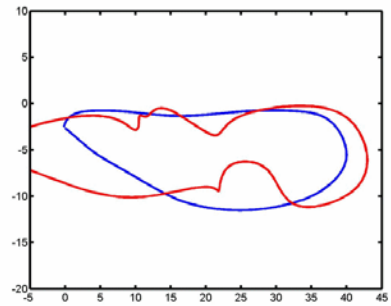
Stingray



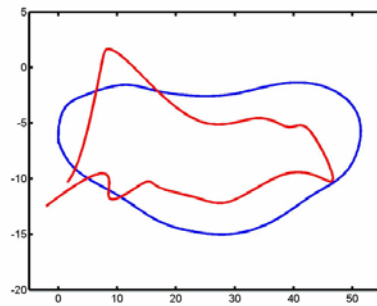
Airfoil



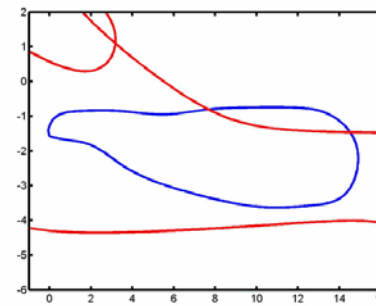
Dragonfly wing-1



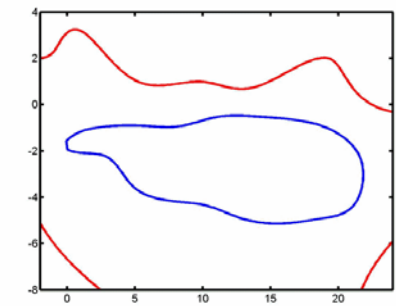
Dragonfly wing-2



Dragonfly wing-3



Damselfly wing-1



Damselfly wing-2

Fig.9 Evolution of generated shape (red) towards the target shape (blue)

- The optimum design of the 3D Flower vase (contains 676 points in x, y and z coordinates) after 100,000 function evaluations.

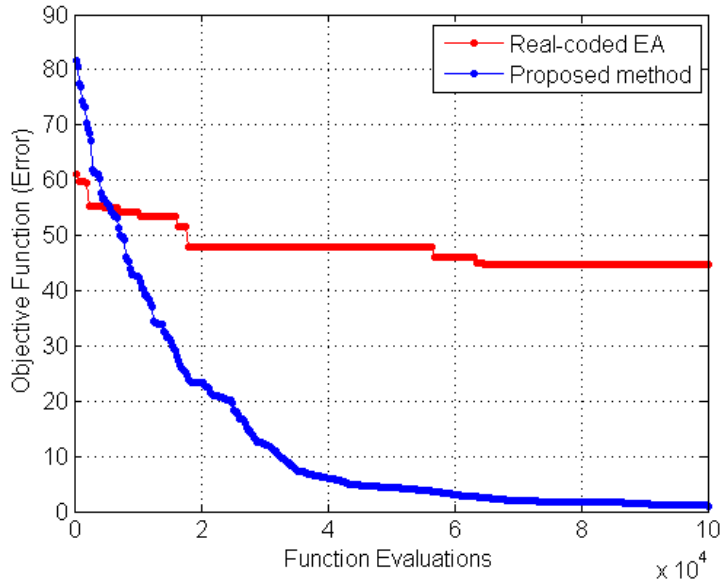
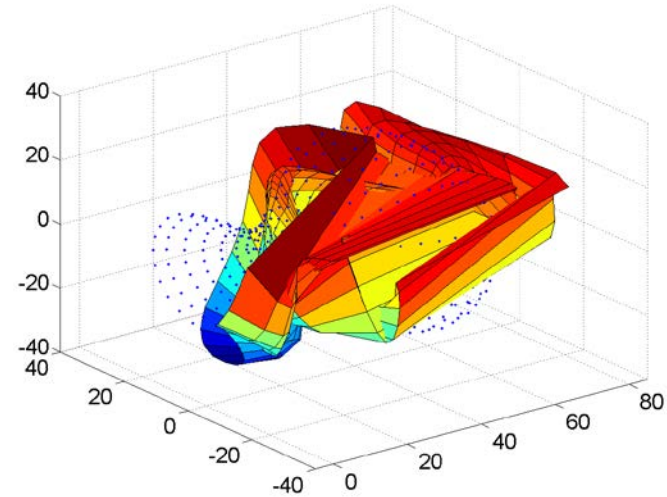


Fig.13 Progress plot of the best design for single objective matching error minimization



Ani.4 Evolution of 3D Flower vase (evolving surface) towards the target Flower vase (point cloud)

| Method | Error Measurement | Best | Worst | Mean | Median | Std. |
|-----------------|-------------------|--------|--------|--------|--------|-------|
| Real-coded EA | Max (Eucli,HD) | 44.694 | 51.002 | 48.324 | 48.043 | 1.627 |
| Proposed method | Max (Eucli,HD) | 0.848 | 1.553 | 1.244 | 1.264 | 0.166 |

Tab. 4 Results for 3D Flower vase shape example

- A 3D ear plug has been considered to support real world product application.
- The evolution of shapes is very crucial component for optimization of shapes according to a patient's ear anatomy and canal.
- The target shape is extracted in the form of a point cloud via a 3D scan.
- The optimum design of the 3D ear plug (contains 841 points in x, y and z coordinates) after 150,000 function evaluations.



Fig. 14 Ear plugs

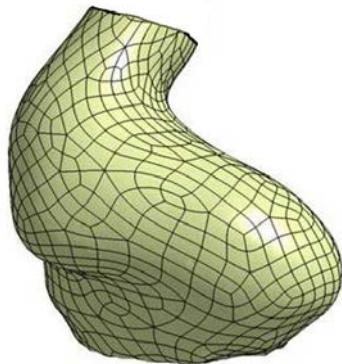


Fig. 15 3D scanned image

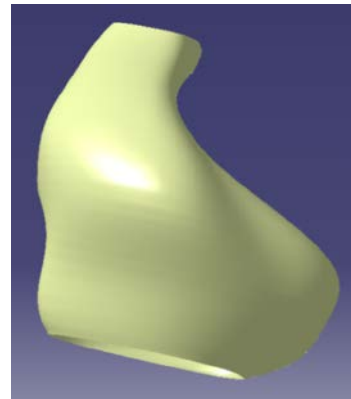
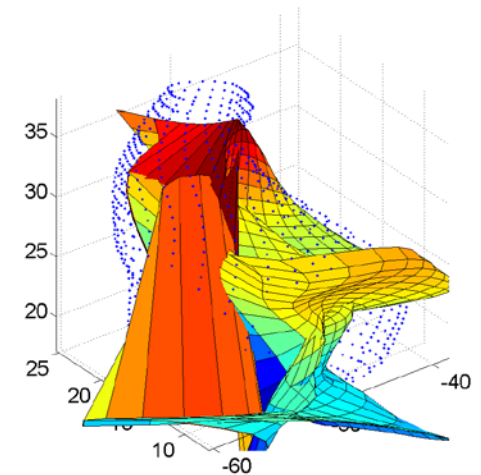


Fig.16 Target shape (CATIA model)



Ani.5 Ear plug evolutions

- The best solutions of the two fidelity models are referred as the **Design-I** (best solution of the empirical-in-loop analysis) and **Design-II** (best solution of the CFD-in-loop analysis) toy submarines.

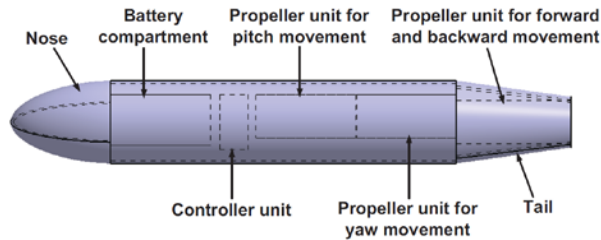


(a) Design-I

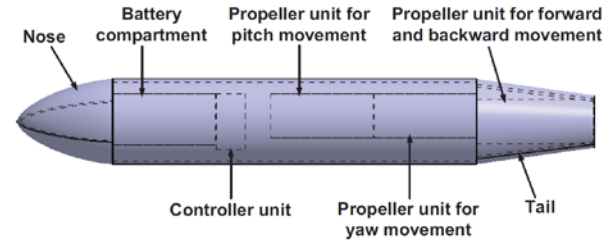


(b) Design-II

Fig. CATIA models of the designed toy submarines

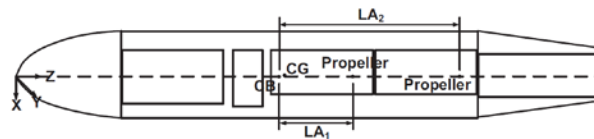


(a) Design-I

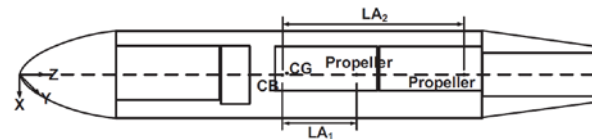


(b) Design-II

Fig. Configurations of the designed toy submarines



(a) Design-I



(b) Design-II

Fig. Longitudinal sections of the designed toy submarines



Fig. Bare hull of the best design

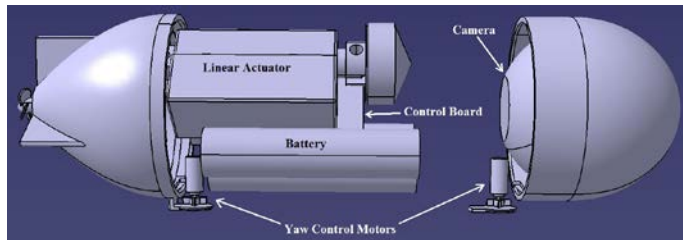
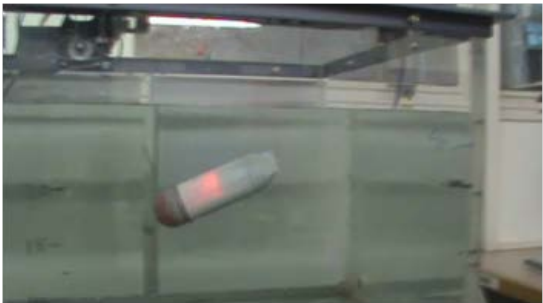
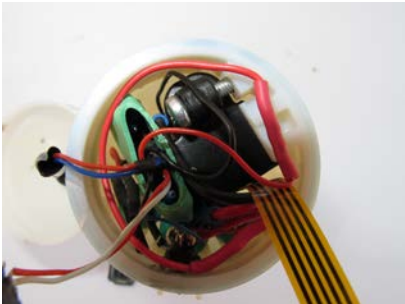
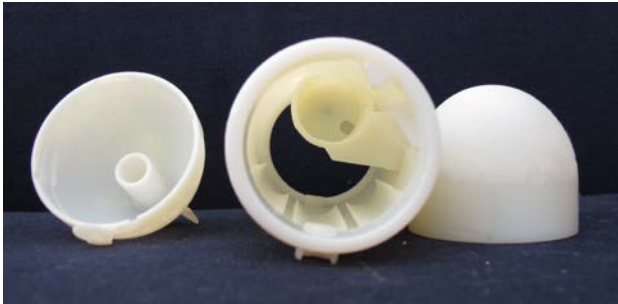


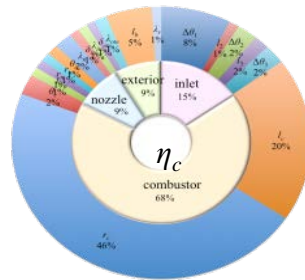
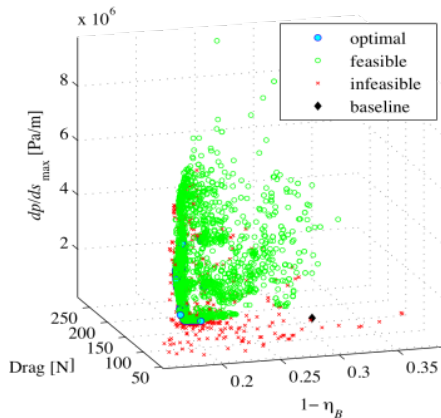
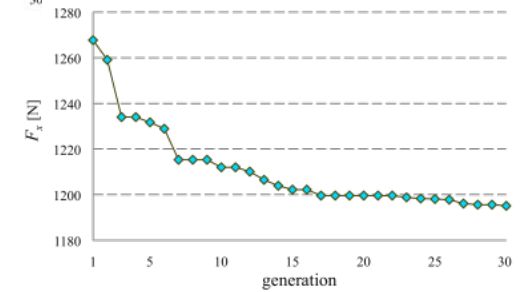
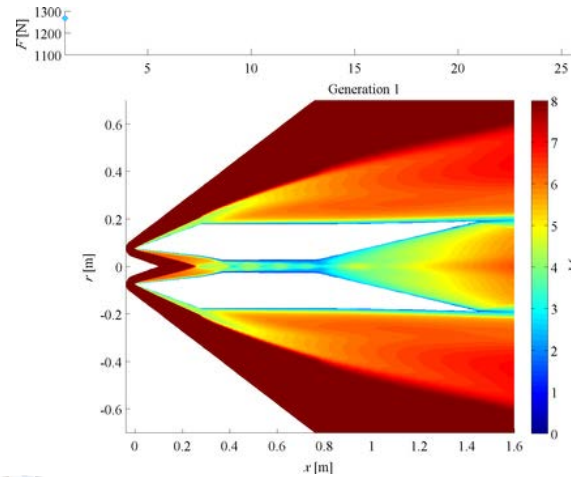
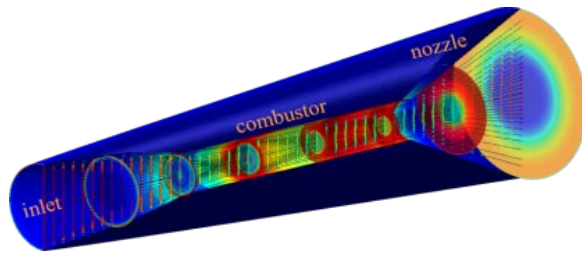
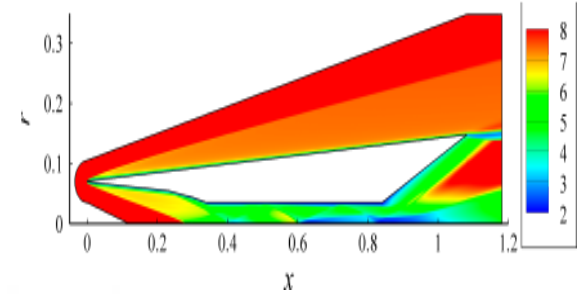
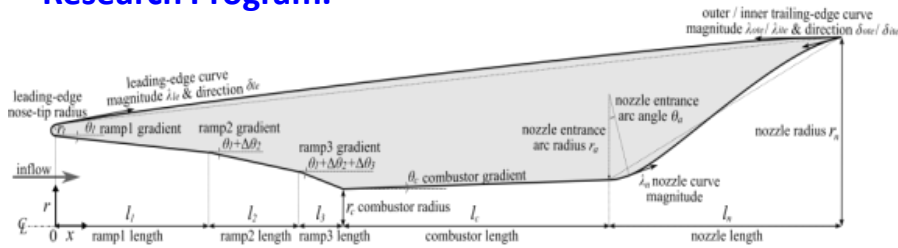
Fig. Internal image of the final design

Table: Performance criteria of the optimized six inch sub

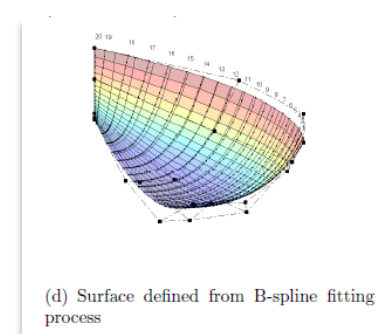
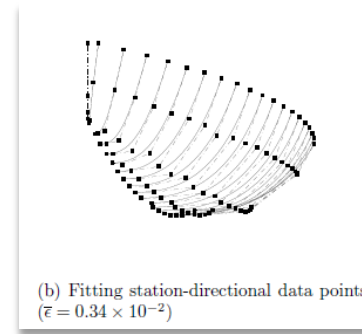
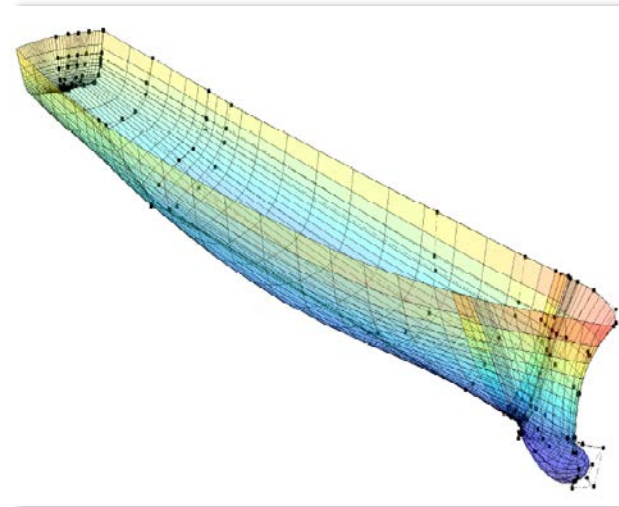
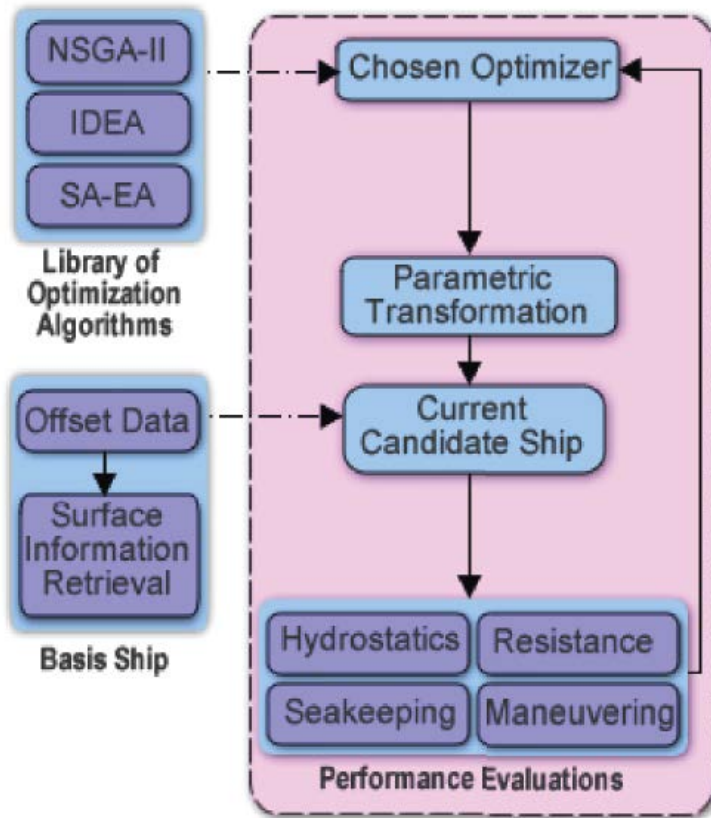
| Vehicle Particulars | | | |
|----------------------|-------------------------|---------------------------|------------|
| Nose length | 40 mm | Total mass of the vehicle | 172.17 g |
| Mid-body length | 78 mm | Max. inner square size | 34.02 mm |
| Tail length | 34.4 mm | First lever arm length | 37.44 mm |
| Length overall | 152.4 mm | Second lever arm length | 38.41 mm |
| Outer diameter | 51.1 mm | CG-CB separation | 3.88 mm |
| L/D ratio | 2.98 | Nominal speed | 0.2 m/s |
| Wetted surface area | 0.021611 m ² | Drag (VT method) | 0.006338 N |
| Displacement volume | 0.000247 m ³ | Drag (G&J method) | 0.006733 N |
| Displaced water mass | 0.247 kg | Drag (MIT method) | 0.008178 N |



Full Flow-Path Design Optimization and Analysis of Axisymmetric Scramjets. Funded by Australian Space Research Program.

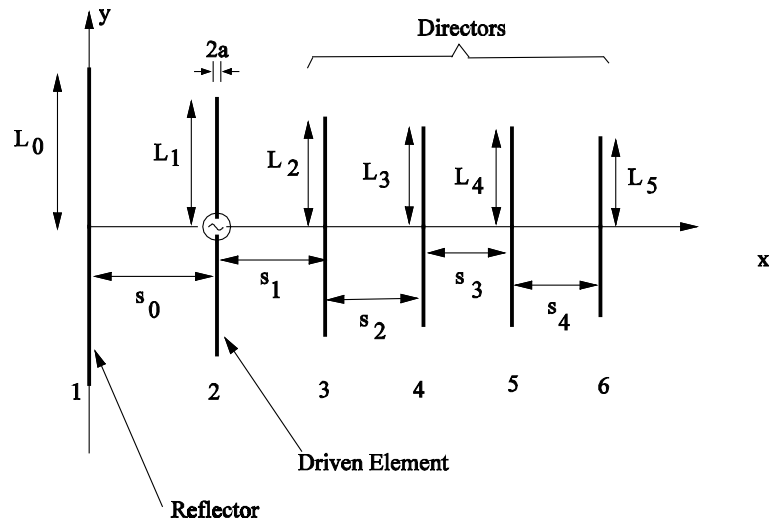


Ogawa, H. Brown, L. Boyce, R.R., and Ray, T., Multiobjective Design Optimization of Axisymmetric Scramjet Nozzle and External Components Considering Static Stability by using Surrogate Assisted Evolutionary Algorithms, International Society of Air-breathing Engines, ISABE 2011, September 12-16, 2011 Gothenburg, Sweden.



1. A library of optimization algorithms
2. Surface information retrieval modules
3. Parametric transformation module
4. Hydrostatics and hydrodynamics module

Mohamad, A.F.A., Ray, T., and Smith, W.(2011), Uncovering Secrets Behind Low Resistance Planing Craft Hull Forms Through Optimization, *Engineering Optimization*.iFirst, 2011, pp. 1-13.

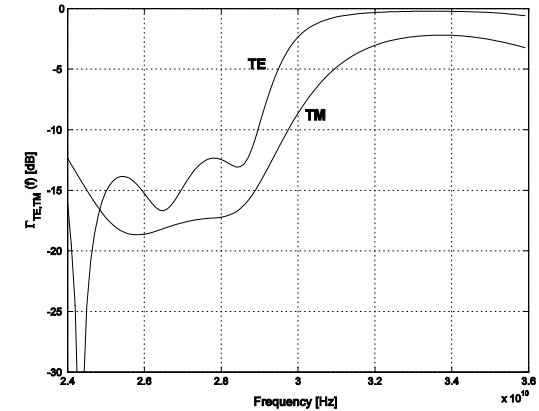
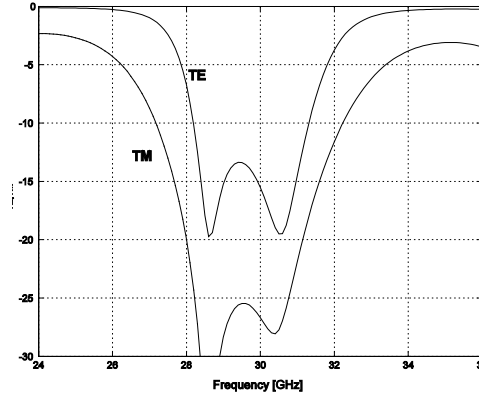
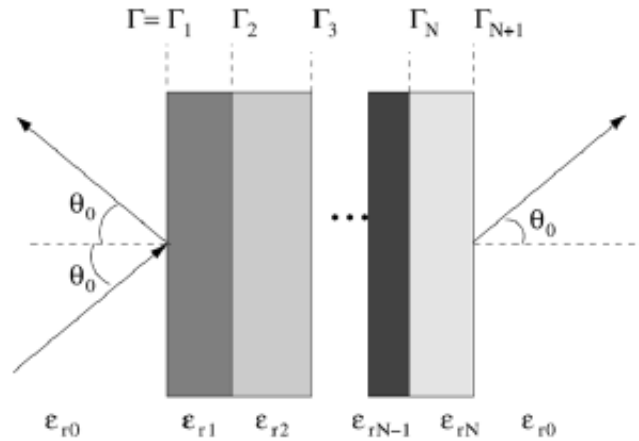


More than 1dBi improvement

TABLE II
15-ELEMENT YAGI-UDA ANTENNA DESIGNS OBTAINED USING (a) GA FROM [7] AND (b) CI ALGORITHM

| Elements | GA optimized [7] | | CI optimized | |
|--------------------------------|------------------|----------------|------------------|----------------|
| | Length, L_n | Spacing, S_n | Length, L_n | Spacing, S_n |
| 1 | 0.236λ | - | 0.235λ | - |
| 2 | 0.230λ | 0.249λ | 0.227λ | 0.196λ |
| 3 | 0.221λ | 0.155λ | 0.224λ | 0.238λ |
| 4 | 0.205λ | 0.185λ | 0.215λ | 0.142λ |
| 5 | 0.216λ | 0.191λ | 0.204λ | 0.231λ |
| 6 | 0.210λ | 0.252λ | 0.212λ | 0.447λ |
| 7 | 0.210λ | 0.442λ | 0.206λ | 0.395λ |
| 8 | 0.189λ | 0.431λ | 0.203λ | 0.371λ |
| 9 | 0.191λ | 0.362λ | 0.201λ | 0.441λ |
| 10 | 0.200λ | 0.205λ | 0.202λ | 0.433λ |
| 11 | 0.204λ | 0.268λ | 0.206λ | 0.445λ |
| 12 | 0.215λ | 0.414λ | 0.196λ | 0.365λ |
| 13 | 0.174λ | 0.197λ | 0.189λ | 0.359λ |
| 14 | 0.199λ | 0.130λ | 0.203λ | 0.429λ |
| 15 | 0.204λ | 0.362λ | 0.196λ | 0.390λ |
| Gain(dBi) | 15.41 | | 16.66 | |
| Z (Ω) | $50.64 - j 5.08$ | | $45.42 - j 5.74$ | |

Venkatrayalu, N. and Ray, T. (2004). Optimum Design of Yagi-Uda Antennas Using Computational Intelligence, *IEEE Trans. On Antennas and Propagation*, Vol. 52, No. 7, pp. 1811- 1818, 2004.



Bandpass Filter Design: Lower cutoff at 28 GHz and Upper cutoff at 32GHz. Reflection coefficient is greater than -5dB in stopband and less than -10dB in the passband. & layered dielectric.

Lowpass Filter Design: Cutoff frequency of 30GHz.

Maximum of 15000 Design Evaluations.

Venkatrayalu, N., Ray, T. and Gan, Y.B., (2005). Multilayer Dielectric Filter Design Using a Multi-objective Evolutionary Algorithm, *IEEE Trans. On Antennas and Propagation*, Vol. 53, No. 11, pp. 3625-3632, 2005.